AAPS PharmSciTech, Vol. 10, No. 4, December 2009 (© 2009)
DOI: 10.1208/s12249-009-9337-8

Research Article

Monitoring Phase Transformations in Intact Tablets of Trehalose by FT-Raman Spectroscopy

Paroma Chakravarty,[1] Sunny P. Bhardwaj,[1] Leslie King,[2] and Raj Suryanarayanan[1,3]

Received 28 July 2009; accepted 7 November 2009; published online 25 November 2009

Abstract. The purpose of this study is to monitor phase transformations in intact trehalose tablets using FT-Raman spectroscopy. Tablets of trehalose dihydrate, amorphous trehalose (obtained by freeze-drying aqueous trehalose solutions), and anhydrous trehalose (β-trehalose) were prepared. The tablets were exposed to different conditions [11% and 0% RH (60°C); 75% RH (25°C)] and monitored periodically over 96 h using Raman spectroscopy. Within 96 h of storage, the following phase transformations were observed: (1) trehalose dihydrate → β-trehalose (11% RH, 60°C), (2) trehalose dihydrate → α-trehalose (0% RH, 60°C), (3) β-trehalose → trehalose dihydrate (75% RH, 25°C), and (4) amorphous trehalose → trehalose dihydrate (75% RH, 25°C). FT-Raman spectroscopy was a useful technique to identify the solid form and monitor multiple-phase transformations in intact trehalose tablets stored at different conditions.

KEY WORDS: phase transformation; Raman spectroscopy; tablet; trehalose.

INTRODUCTION

Raman spectroscopy is a widely used technique for the physical characterization of pharmaceutical solids. Although often used as a complement to infrared (IR) spectroscopy, Raman analysis offers some distinct advantages. Since sample preparation is not required, Raman spectroscopy is the method of choice for analyzing intact solid dosage forms (tablets and capsules). Spectral changes are readily detected since the peaks are usually sharp and well resolved. Pharmaceutical actives containing aromatic heterocyclic groups can be easily distinguished, even when present at low concentrations, from commonly used partially amorphous excipients which are poor Raman scatterers (1). Moreover, water is a weak Raman scatterer but produces a very strong IR signal in the 3,500–3,000 cm^{-1} wavenumber region of the spectrum. Therefore, Raman spectroscopy is the method of choice to monitor solid-state transformations in aqueous slurries (2).

Molecules of pharmaceutical interest often contain one or more aromatic heterocyclic rings giving rise to characteristic C—H and C—C stretching as well as highly symmetrical vibrational modes which make them particularly amenable to Raman spectroscopic analysis (3). In the present study, α,α-trehalose(α-D-glucopyranosyl α-D-glucopyranoside) has been used as a model compound to monitor solid-state transformations in intact compacts. Trehalose is a disaccharide and is extensively used as a lyoprotectant in freeze-dried formulations (4). This sugar is commercially available, both in the crystalline anhydrous state (β-trehalose, T_β) and as a dihydrate ($C_{12}H_{22}O_{11}.2H_2O$; T_H). A second anhydrous form of trehalose, the "dehydrated dihydrate" or α-trehalose (T_α), may be obtained by slow dehydration of the dihydrate at low temperatures (≤60°C). Amorphous trehalose (T_a) is typically obtained by freeze-drying or spray-drying an aqueous trehalose solution and has a glass transition temperature of ~117°C (5). All the four solid forms of trehalose have been extensively characterized (5–16). Raman spectroscopy can be used to distinguish between these different physical forms of trehalose based on the differences in the positions and intensities of peaks attributed to: (1) asymmetrical and symmetrical vibrational stretchings of the ring C—H (3,015–2,880 cm^{-1}), (2) vibrations in the 900–750 cm^{-1} region due to conformation of the anomeric carbon, and (3) vibrations from the glucose bands in the 700–200 cm^{-1} region.

Trehalose was selected as a model compound since there are several physical forms of trehalose and the stability of these forms is strongly dependent on the environmental conditions (4,5,9,10,13,14,16). The nature of the product phase (the physical form as well as its crystallinity) can be strongly influenced by the dehydration conditions of trehalose dihydrate. The primary aim of our study was to use FT-Raman spectroscopy as a rapid and nondestructive technique to identify the physical form of trehalose in *intact* tablets and monitor the effect of storage conditions on the physical form of trehalose in intact tablets. We have focused on the different solid-state transformations observed in trehalose (hydrate → anhydrate, amorphous → hydrate, hydrate → "dehydrated hydrate," anhydrate → hydrate) to highlight the utility of

[1] Department of Pharmaceutics, University of Minnesota, 9-157 Weaver Densford Hall, 308 Harvard Street SE, Minneapolis, Minnesota 55455, USA.
[2] Lilly Research Labs, Eli Lilly and Company, Indianapolis, Indiana 46221, USA.
[3] To whom correspondence should be addressed. (e-mail: surya001@umn.edu)

Raman spectroscopy in distinguishing these forms. In addition, X-ray powder diffractometry (XRPD), thermogravimetry, and water sorption studies were used to characterize the different physical forms of trehalose. In selected instances, tablets were crushed and subjected to XRPD so as to obtain "bulk" information.

MATERIALS AND METHODS

Materials

α,α-Trehalose was obtained in the anhydrous form (β-polymorph; T_β) and as trehalose dihydrate (T_H) from ACROS Organics (New Jersey, USA) and used as received. amorphous trehalose (T_a) was obtained by freeze-drying an aqueous trehalose solution (10% *w*/*v*) by slightly modifying the method described by Rani *et al.* (5). Secondary drying was conducted at 40°C for 24 h. T_a so obtained was stored at 60°C (oven) for 4 h and the final water content, determined by thermogravimetry, was ~3% *w*/*w*. T_α was obtained by dehydrating T_H at 60°C (5).

Methods

Water Sorption

About 17 mg of T_β was placed in the quartz sample pan of an automated vapor sorption analyzer (SGA-100, VTI Corporation, Hialeah, FL), maintained at 25°C. The sample was equilibrated at 0% RH for 100 min, and then the RH was progressively increased, in 10% increments, to 80% with a hold time of 100 min at each step. This was followed by progressive lowering of the RH in 10% decrements, to 0% with the same hold time. The weight gain at the end of the sorption cycle (80% RH) was calculated on the basis of the dry weight.

Tablet Preparation and Storage

T_H, T_β, and T_a powders were passed through a Standard ASTM sieve # 60 (particle size <250 μm). The powder was weighed (200 mg) and compressed to 112–126 MPa on an automated hydraulic Press (Fred S. Carver Inc, Menomonee Falls, WI) and held for 10 s. The tablets were stored over saturated salt solutions, at 25°C and 60°C, to maintain the desired RH (sodium chloride solution—75% RH (25°C), lithium chloride solution—11% RH (60°C), anhydrous $CaSO_4$—~0% RH). T_H tablets were stored at 0% and 11% RH (60°C) while T_β and T_a tablets were stored at 75% RH (25°C).

FT-Raman and NIR Spectroscopy

Powder samples of T_H, T_α, T_β, and T_a were sealed in glass vials under nitrogen purge to prevent exposure to ambient environment during data acquisition. The spectra were recorded using a FT-Raman system (Vertex 70 with Raman II Module, Bruker, Billerica, MA) equipped with a 500-mW diode pumped Nd:YAG laser operating at 1,064 nm as the excitation source. Backscattered radiation was collected using a liquid nitrogen-cooled germanium detector. The laser power was 301 mW. For each spectrum, 32 scans were collected and the collection time was approximately 1 min. Tablets of T_H, T_β, and T_a were analyzed right after preparation ($n \geq 3$). The stored tablets were analyzed periodically over 96 h. In each tablet, at least four to five spots were sampled on the tablet surface through sealed glass vials. The data were processed using OPUS® software (version 5.5, Bruker Optics). In addition to FT-Raman, near infrared (NIR) spectra of the powder samples of T_H, T_α, T_β, and T_a were collected using a Spectral Dimensions NIR-Cl 2450 spectrometer (Malvern Inc., MA).

RESULTS

Figure 1a contains the Raman spectra of T_H, T_α, T_β, and T_a. These forms were also characterized by X-ray diffractometry. The XRPD patterns of the four physical forms of trehalose were in excellent agreement with published data and have, therefore, not been shown (5). Figure 1b shows the NIR spectra of these forms.

The Raman spectra, in the wavenumber range of 950 to 810 cm^{-1}, are shown in Fig. 2 and highlight the major

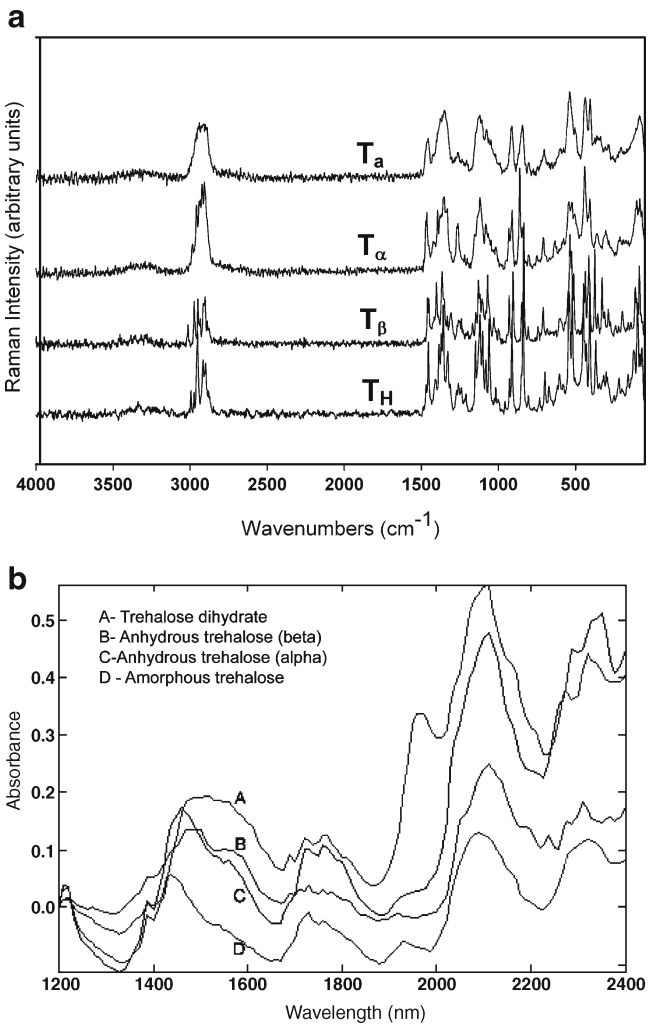

Fig. 1. **a** Raman spectra of amorphous trehalose (T_a), α-trehalose (T_α) (also referred to as "dehydrated dihydrate"), anhydrous β-trehalose (T_β), and trehalose dihydrate T_H. **b** NIR spectra of the different solid-state forms of trehalose

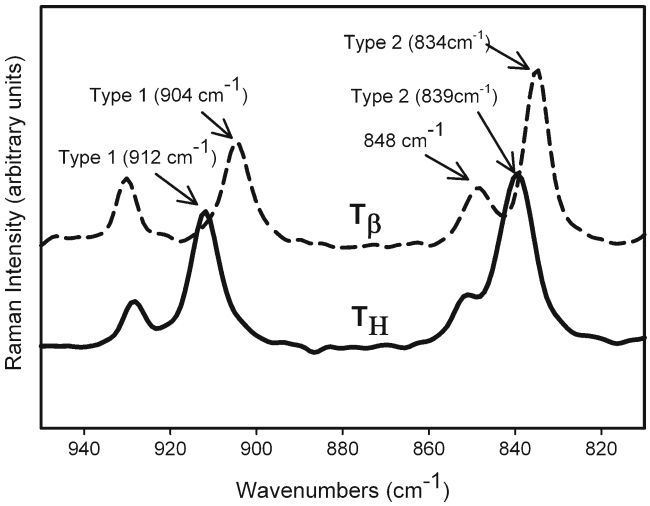

Fig. 2. Raman spectra of T_H and T_β. The types 1 and 2 bands are indicated

differences in the spectra of T_H and T_β. The peaks represent vibrations arising from conformation of the anomeric carbon. The position and relative intensity of types 1 and 2 bands (arising due to the α-conformation of the glycosidic linkage of the anomeric carbon at 912 and 839 cm^{-1}, respectively) differ in T_β from that in T_H. There is a shift in peak position of the type 1 band from 912 in T_H to 904 cm^{-1} in T_β. The type 2 band also shifts to a lower wavenumber in T_β and the shoulder on this band (as seen in T_H) shapes into a peak at 848 cm^{-1} (4).

Figure 3 shows the spectra of T_H and T_a in two regions—3,075–825 and 1,525–890 cm^{-1}. The peaks in T_a are broader and poorly resolved compared to those in crystalline trehalose (T_H). Since the conformation in the glycosidic linkage in trehalose is relatively inflexible, the bands (Type 1 at 912 cm^{-1} and 2 at 839 cm^{-1}) arising due to its vibration are seen at approximately the same position in T_a and T_H (4).

Figure 4 highlights the spectral differences between T_H, T_β, and T_α in the 1,000–800 cm^{-1} region. The peak at 863 cm^{-1} is unique to T_α and is not present in either T_β or T_H (17). Our spectrum is substantially similar to that reported by Gil *et al.* (17,18). The observed minor differences from the reported spectrum can be attributed to the differences in crystallinity, likely brought about by the method of preparation of T_α. We had earlier pointed out that the degree of crystallinity of T_α is strongly influenced by its method of preparation (5).

$T_\beta \rightarrow T_H$ Transformation (Hydration of Crystalline Anhydrate)

Figure 5 shows the representative Raman spectra of T_β tablets stored at 75% RH (25°C) up to 12 h. The 950–820 cm^{-1} range is highlighted in the inset. The spectra of pure forms (T_H and T_β) are provided for comparison. After 6 h of storage, a shoulder appeared in the T_β peak at 904 cm^{-1} which corresponded to the type 1 peak of T_H at 912 cm^{-1}. By 10 h, the type 1 peak of T_H formed completely and the type 2 band shifted to a higher wavenumber, with a small shoulder characteristic of T_H. The spectra obtained at ≥10 h of storage of T_β (75% RH, 25°C) were identical to that of T_H.

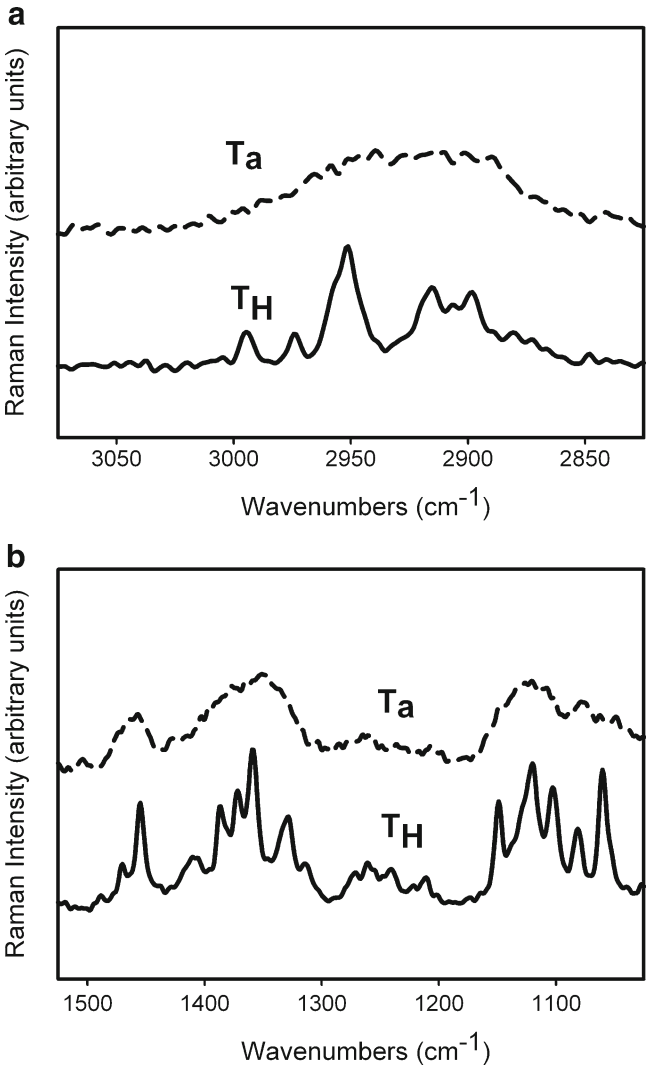

Fig. 3. Raman spectra of T_H and T_a in the **a** 3,075–2,825 and **b** 1,525–890 cm^{-1} spectral range. The spectrum of T_H shows sharp, well resolved peaks while T_a is characterized by broad peaks

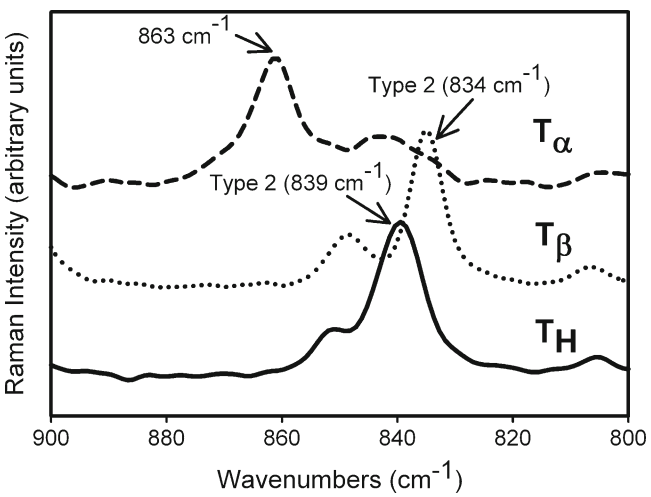

Fig. 4. Raman spectra of T_H, T_β, and T_α in the 900–800 cm^{-1} spectral range. The type 2 bands of T_H and T_β are indicated. The peak at 863 cm^{-1} is unique to T_α

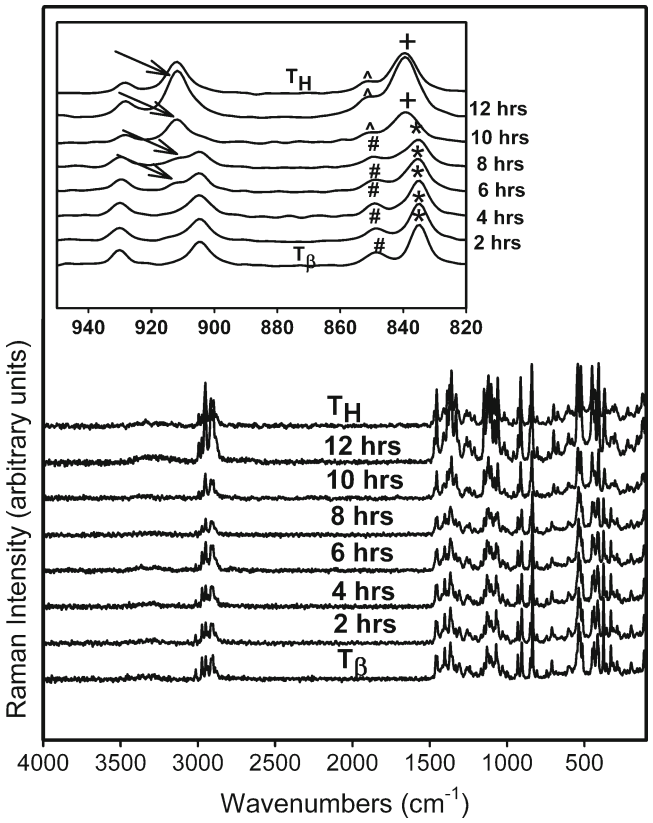

Fig. 5. Raman spectra collected periodically following storage of T_β at 75% RH (25°C). The spectra of T_H and T_β are provided for comparison. The 950–820 cm^{-1} spectral range is magnified in the inset. Type 1 band of T_H (→) appeared at 6 h of storage. At 10 h, (1) the type 2 band of T_β (*asterisk*) shifted to a higher wavenumber reflecting the appearance of the type 2 band of T_H (*plus sign*), and (2) the peak at 848 cm^{-1} (*number sign*) in T_β is reduced to a shoulder in T_H (*caret*)

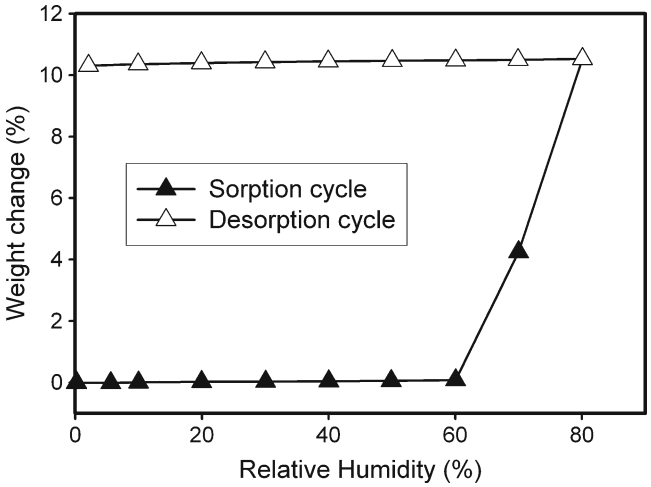

Fig. 6. Water sorption–desorption profile of T_β (25°C). The sample was equilibrated at 0% RH for 100 min, and then the RH was progressively increased in steps of 10% RH to 80%, with a hold time of 100 min at each step. The RH was then progressively lowered in decrements of 10% to 0% RH with 100 min of hold time at every step. The weight gain, at the end of the sorption cycle (80% RH), was calculated on the basis of the dry weight at 0% RH

The $T_\beta \rightarrow T_H$ transformation at 75% RH was also confirmed by water sorption of T_β at 25°C. Figure 6 shows the water sorption–desorption profile of T_β. At RH>60%, the observed weight gain indicated T_H formation. When the RH was then progressively lowered to 0%, the negligible weight loss indicated that T_H did not dehydrate in the experimental time scale.

$T_a \rightarrow T_H$ Transformation (Crystallization of Amorphous Trehalose to Dihydrate)

Figure 7 contains the Raman spectra of T_a tablets stored at 75% RH (25°C). The 3,050–2,850-cm^{-1} range, highlighted in the inset, reveals the appearance of T_H. After storage for 30 h, a sharp characteristic peak of T_H at 2,952 cm^{-1} was observed (Fig. 7 inset). From then on, $T_a \rightarrow T_H$ transformation progressed rapidly and by 49 h, almost all the T_H peaks appeared. Our results are in agreement with the reported crystallization of T_a at RH≥50% (25°C) (5).

$T_H \rightarrow T_\beta$ Transformation (Dehydration to Crystalline Anhydrate)

Figure 8 shows representative Raman spectra of T_H tablets stored at 11% RH (60°C) for 96 h. The spectral range of 950–820 cm^{-1} is highlighted in the inset. The spectra of pure forms (T_H and T_β) are provided for comparison. Although there are literature reports of dehydration of T_H to form T_β when heated under humid conditions (~60% RH

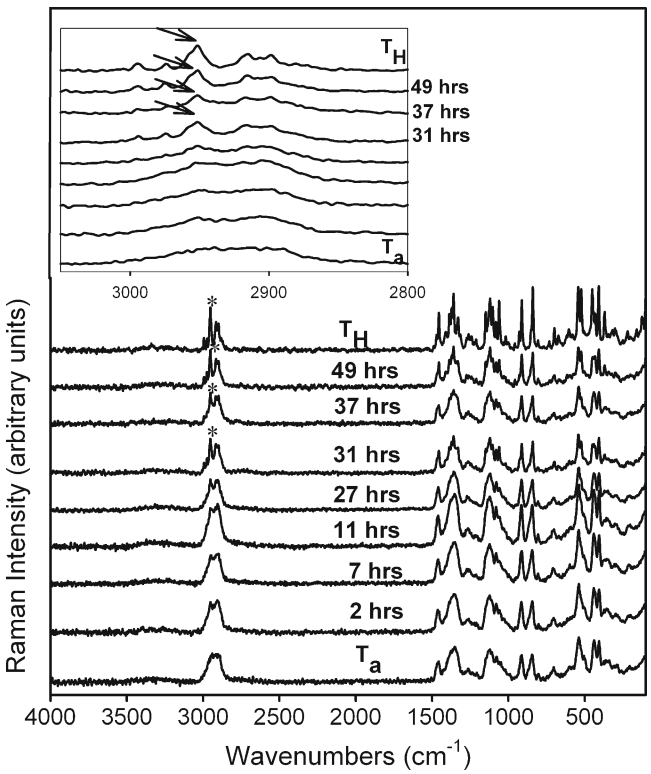

Fig. 7. Raman spectra collected periodically following storage of T_a at 75% RH (25°C). The spectra of T_H and T_a are provided for comparison. The 3,050–2,850 cm^{-1} range has been highlighted in the *inset* to indicate the appearance of T_H peaks. In the spectra acquired following storage for 31 h, the crystallization of T_H was evident from the increase in intensity and resolution of characteristic T_H peaks. The peak at 2,952 cm^{-1} is a representative example (*arrows*)

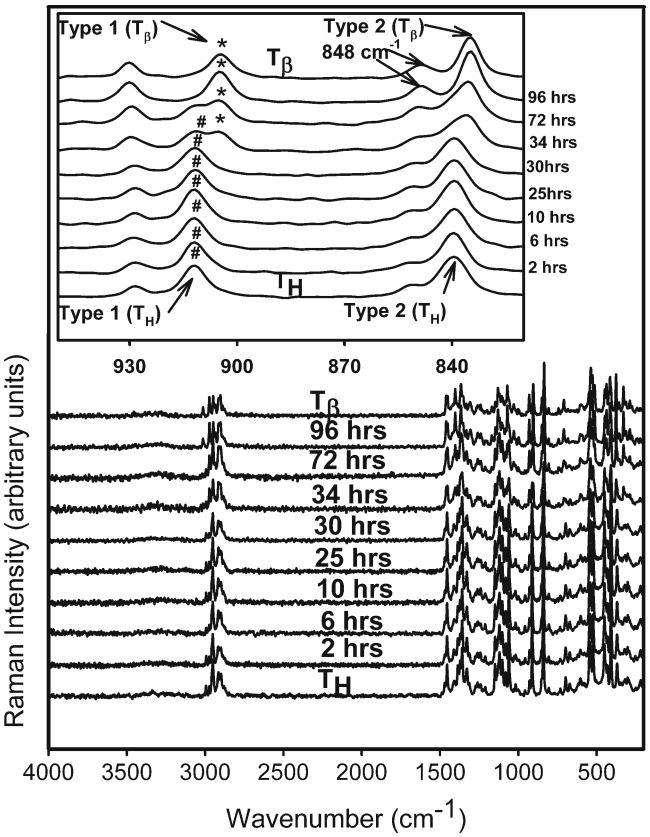

Fig. 8. Raman spectra collected periodically following storage of T_H at 11% RH (60°C). The spectra of T_H and T_β are provided for comparison. The 950–820 cm^{-1} range has been highlighted in the *inset*. The type 1 band of T_β appeared at 34 h of storage. At the same time, the type 2 band of T_H shifted to a lower wavenumber (characteristic of T_β) and its shoulder developed into a peak at 848 cm^{-1}

at 60°C) or upon exposure to 20% RH (60°C) for several hours (5,19), our results indicate that $T_H \rightarrow T_\beta$ transition occurs even at lower water vapor pressures (at 60°C). Furuki *et al.* have provided a "bridge-effect" mechanism to explain this phase conversion (19). Presence of moisture in the surrounding environment of T_H acts as an eluant to extract water and "traps" the released water by means of hydrogen bonds. This surrounding moisture layer prevents the lattice from complete collapse and allows for molecular reorganization in the lattice. However, since $T_H \rightarrow T_\beta$ transformation requires conversion from a rhombic to a monoclinic lattice, the transformation kinetics is dependent on both temperature and water vapor pressure (19). This may explain the long time required for the complete $T_H \rightarrow T_\beta$ transformation in T_H tablets (tablet surface).

$T_H \rightarrow T_\alpha$ Transformation (Dehydration to "Dehydrated" Hydrate)

Figure 9 shows the Raman spectra, in the 4,000–20 cm^{-1} spectral range, of T_H stored at 0% RH (60°C). The 900–800 cm^{-1} region is highlighted in the inset. The gradual loss in spectral features suggests a decrease in crystallinity. The appearance of the peak at 863 cm^{-1} (inset) at 2 h indicated the formation of T_α. After storage for 6 h, the formation of T_α appeared to be complete. The $T_H \rightarrow T_\alpha$ transformation was also observed in powder samples stored at 60°C (under nitrogen purge) for 5 h. T_α so formed, while partially crystalline, retains some of the hydrate lattice structure (5).

X-ray Powder Diffractometry

Powdered trehalose tablets (T_H, T_β and T_a) were subjected to X-ray powder diffractometry after 4 days of storage at: 25°C/75% RH, 60°C/0% RH, and 60°C/11% RH. The phase transformations observed (data not shown) were the same as by Raman spectroscopy. Since the XRPD studies were conducted on powdered tablets, these results are believed to reflect the phase composition of the "bulk." It is, therefore, reasonable to assume that the transformation occurred throughout the tablet.

DISCUSSION

We have demonstrated the use of FT-Raman spectroscopy to monitor multiple phase transformations in intact solid dosage forms. The storage conditions, selected based on earlier work on powder samples, facilitated the desired phase transformations in the time scale of hours and days. Other selected applications of Raman spectroscopy in pharmaceutical systems are listed below. (1) Characterization of the physical form of pharmaceuticals (including formulation components), specifically, polymorphic form, state of solvation, and the degree of crystallinity (20–25). (2) Quantification of secondary protein structure (monoclonal antibody)

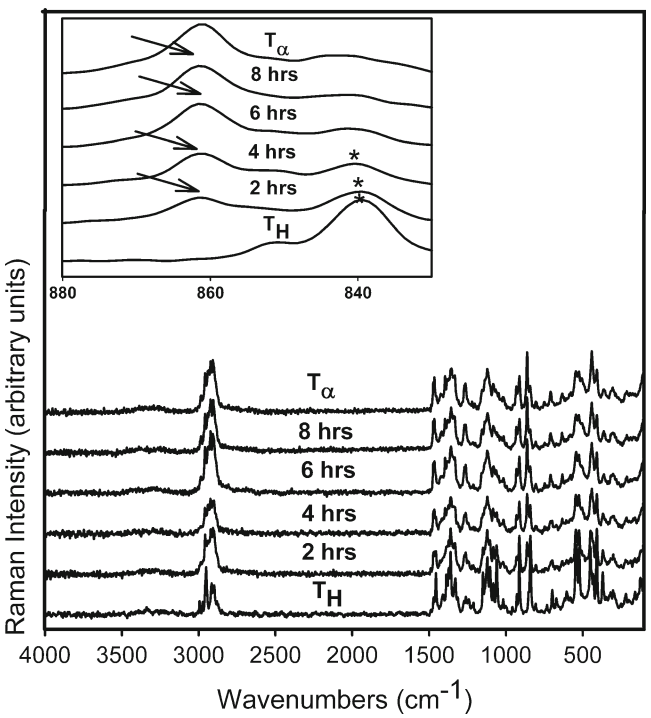

Fig. 9. Raman spectra collected periodically following storage of T_H at 0% RH (60°C). The spectra of T_H and T_α are provided for comparison. The 880–800 cm^{-1} range has been highlighted in the *inset*. The characteristic peak of T_α (*arrow*) at 863 cm^{-1} was observed at 2 h. The $T_H \rightarrow T_\alpha$ transition appears to be complete in 8 h

both in solution and in solid-state (26). (3) Chemical form analysis such as determination of tablet composition and impurity identification (27). (4) API quantification in microspheres, suspensions, and capsules (28,29). (5) Quantification of formulation components in packaged formulations (blister packing) (28). (6) Process monitoring (identification and quantification) of physical form of API during high-shear wet granulation (30,31). The increasingly effective "in-line" use of Raman spectroscopy in form analysis (both qualitative and quantitative) in pharmaceutical unit operations has brought to light its potential as a valuable process analytical technology tool in the pharmaceutical industry.

Despite its wide usage, one of the drawbacks of this technique is that it is ideally suited to monitor the surfaces of solid samples. The depth of penetration depends on many factors including the power source, wavelength of excitation, and sample material properties. Though systematic studies were not conducted to determine the depth of penetration, the reported phase information has a considerable surface bias. This is because of the instrumentation parameters as well as the use of compacts (32). XRPD was, therefore, used as a complementary technique to obtain "bulk" information by analyzing the crushed tablets.

Although the present study focused on characterizing a single component dosage form, our results can be readily extended to multicomponent formulations. Since a large fraction of commonly used pharmaceuticals excipients do not exhibit characteristic peaks in the CH stretching region, characterization of the different physical forms of trehalose will be unaffected.

CONCLUSION

In trehalose tablets, the storage conditions (temperature, water vapor pressure) dictate phase transformations ($T_\beta \rightarrow T_H$, $T_\mathrm{a} \rightarrow T_\mathrm{H}$, $T_H \rightarrow T_\beta$, and $T_H \rightarrow T_\alpha$). These transformations, in intact tablets, were monitored by FT-Raman spectroscopy. X-ray diffractometry of powdered tablet samples, confirmed the transformations observed by Raman spectroscopy. Thus, by combining the two techniques, transformations in the tablet surface and bulk were monitored.

ACKNOWLEDGEMENTS

We thank Kurt Schlegel for freeze-drying trehalose, Gregory Clanton for the water sorption studies and X-ray diffractometry data acquisition, and Edward McCarty for assistance with tabletting. Drs. Nathanial Milton, Gregory Stephenson, and David Moeckly are gratefully acknowledged for their support. A part of the work was carried out by PC during a summer internship at Eli Lilly and Company.

REFERENCES

1. Taylor LS, Langkilde FW. Evaluation of solid-state forms present in tablets by Raman spectroscopy. J Pharm Sci. 2000;89 (10):1342–53.
2. Strachan CJ, Rades T, Gordon KC, Rantanen J. Raman spectroscopy for quantitative analysis of pharmaceutical solids. J Pharm Pharmacol. 2007;59(2):179–92.
3. Williams AC. Some pharmaceutical applications of Raman spectroscopy. In: Lewis IR, Edwards HGM, editors. Handbook of Raman spectroscopy. New York: Marcel Dekker; 2001. p. 575–91.
4. Taylor LS, Williams AC, York P. Particle size dependent molecular rearrangements during the dehydration of trehalose dihydrate. *In situ* FT-Raman spectroscopy. Pharm Res. 1998;15 (8):1207–14.
5. Rani M, Govindarajan R, Surana R, Suryanarayanan R. Structure in dehydrated trehalose dihydrate-evaluation of the concept of partial crystallinity. Pharm Res. 2006;23(10):2356–67.
6. Nagase H, Endo T, Ueda H, Nagai T. Influence of dry conditions on dehydration of alpha, alpha -trehalose dihydrate. STP Pharma Sci. 2003;13(4):269–75.
7. Nagase H, Endo T, Ueda H, Nakagaki M. An anhydrous polymorphic form of trehalose. Carbohydr Res. 2002;337 (2):167–73.
8. Nagase H, Ogawa N, Endo T, Shiro M, Ueda H, Sakurai M. Crystal structure of an anhydrous form of trehalose: structure of water channels of trehalose polymorphism. J Phys Chem B. 2008;112(30):9105–11.
9. Sussich F, Bortoluzzi S, Cesaro A. Trehalose dehydration under confined conditions. Thermochim Acta. 2002;391(1–2):137–50.
10. Sussich F, Cesaro A. Transitions and phenomenology of alpha, alpha-trehalose polymorphs inter-conversion. J Therm Anal Calorim. 2000;62(3):757–68.
11. Sussich F, Cesaro A. Trehalose amorphization and recrystallization. Carbohydr Res. 2008;343(15):2667–74.
12. Sussich F, Skopec C, Brady J, Cesaro A. Reversible dehydration of trehalose and anhydrobiosis: from solution state to an exotic crystal? [Erratum to document cited in CA136:37830]. Carbohydr Res. 2003;338(11):1259.
13. Sussich F, Urbani R, Cesaro A, Princivalle F, Bruckner S. New crystalline and amorphous forms of trehalose. Carbohydr Lett. 1997;2(6):403–8.
14. Sussich F, Urbani R, Princivalle F, Cesaro A. Polymorphic amorphous and crystalline forms of trehalose. J Am Chem Soc. 1998;120(31):7893–9.
15. Taga T, Senma M, Osaki K. Crystal and molecular structure of trehalose dihydrate. Acta Crystallogr, Sect B. 1972;28(Pt. 11):3258–63.
16. Taylor LS, York P. Characterization of the phase transitions of trehalose dihydrate on heating and subsequent dehydration. J Pharm Sci. 1998;87(3):347–55.
17. Gil AM, Belton PS, Felix V. Spectroscopic studies of solid alpha–alpha trehalose. Spectrochim Acta A. 1996;52A(12):1649–59.
18. Belton PS, Gil AM. IR and Raman spectroscopic studies of the interaction of trehalose with hen egg white lysozyme. Biopolymers. 1994;34(7):957–61.
19. Furuki T, Kishi A, Sakurai M. De- and rehydration behavior of alpha, alpha -trehalose dihydrate under humidity-controlled atmospheres. Carbohydr Res. 2005;340(3):429–38.
20. Kontoyannis CG. Quantitative determination of calcium carbonate and glycine in antacid tablets by laser Raman spectroscopy. J Pharm Biomed Anal. 1995;13(1):73–6.
21. Langkilde FW, Sjoeblom J, Tekenbergs-Hjelte L, Mrak J. Quantitative FT-Raman analysis of two crystal forms of a pharmaceutical compound. J Pharm Biomed Anal. 1997;15 (6):687–96.
22. Orkoula MG, Kontoyannis CG. Non-destructive quantitative analysis of risperidone in film-coated tablets. J Pharm Biomed Anal. 2008;47(3):631–5.
23. Szep A, Marosi G, Marosfoei B, Anna P, Mohammed-Ziegler I, Viragh M. Quantitative analysis of mixtures of drug delivery system components by Raman microscopy. Polym Adv Technol. 2003;14(11–12):784–9.
24. Taylor LS, Zografi G. The quantitative analysis of crystallinity using FT-Raman spectroscopy. Pharm Res. 1998;15(5):755–61.
25. Tian F, Zeitler JA, Strachan CJ, Saville DJ, Gordon KC, Rades T. Characterizing the conversion kinetics of carbamazepine polymorphs to the dihydrate in aqueous suspension using Raman spectroscopy. J Pharm Biomed Anal. 2006;40(2):271–80.
26. Sane SU, Wong R, Hsu CC. Raman spectroscopic characterization of drying-induced structural changes in a therapeutic antibody: correlating structural changes with long-term stability. J Pharm Sci. 2004;93(4):1005–18.

27. King TH, Mann CK, Vickers TJ. Determination of phenylpropanolamine hydrochloride and acetaminophen in pharmaceutical preparations by Raman spectroscopy. J Pharm Sci. 1985;74 (4):443–7.
28. Niemczyk TM, Delgado-Lopez MM, Allen FS. Quantitative determination of bucindolol concentration in intact gel capsules using Raman spectroscopy. Anal Chem. 1998;70(13):2762–5.
29. Watts PJ, Tudor A, Church SJ, Hendra PJ, Turner P, Melia CD, *et al.* Fourier transform-Raman spectroscopy for the qualitative and quantitative characterization of sulfasalazine-containing polymeric microspheres. Pharm Res. 1991;8(10):1323–8.
30. Wikstrom H, Carroll WJ, Taylor LS. Manipulating theophylline monohydrate formation during high-shear wet granulation through improved understanding of the role of pharmaceutical excipients. Pharm Res. 2008;25(4):923–35.
31. Wikstrom H, Marsac PJ, Taylor LS. In-line monitoring of hydrate formation during wet granulation using Raman spectroscopy. J Pharm Sci. 2005;94(1):209–19.
32. Kogermann K, Zeitler JA, Rantanen J, Rades T, Taday PF, Pepper M, *et al.* Investigating dehydration from compacts using terahertz pulsed, Raman, and near-infrared spectroscopy. Appl Spectrosc. 2007;61(12):1265–74.